Adipose Stem Cell Treatment in Mice Attenuates Lung and Systemic Injury Induced by Cigarette Smoking

Kelly S. Schweitzer[1,2], Brian H. Johnstone[3,4], Jana Garrison[1,2], Natalia I. Rush[1,2], Scott Cooper[5], Dmitry O. Traktuev[3,4], Dongni Feng[3,4], Jeremy J. Adamowicz[1,2], Mary Van Demark[1,2], Amanda J. Fisher[2,6], Krzysztof Kamocki[2,7], Mary Beth Brown[1,2], Robert G. Presson, Jr.[2,6], Hal E. Broxmeyer[4,5], Keith L. March[3,4,8]*, and Irina Petrache[1,2,4,8]*

[1]Division of Pulmonary and Critical Care Medicine, [2]Center for Immunobiology, [3]Division of Cardiology, [4]Indiana Center for Vascular Biology and Medicine and VC-CAST Signature Center, [5]Department of Microbiology and Immunology, [6]Department of Anesthesiology, [7]Department of Biochemistry and Molecular Biology, and [8]Roudebush Veteran Affairs Medical Center, Indiana University, Indianapolis, Indiana

Rationale: Adipose-derived stem cells express multiple growth factors that inhibit endothelial cell apoptosis, and demonstrate substantial pulmonary trapping after intravascular delivery.

Objectives: We hypothesized that adipose stem cells would ameliorate chronic lung injury associated with endothelial cell apoptosis, such as that occurring in emphysema.

Methods: Therapeutic effects of systemically delivered human or mouse adult adipose stem cells were evaluated in murine models of emphysema induced by chronic exposure to cigarette smoke or by inhibition of vascular endothelial growth factor receptors.

Measurements and Main Results: Adipose stem cells were detectable in the parenchyma and large airways of lungs up to 21 days after injection. Adipose stem cell treatment was associated with reduced inflammatory infiltration in response to cigarette smoke exposure, and markedly decreased lung cell death and airspace enlargement in both models of emphysema. Remarkably, therapeutic results of adipose stem cells extended beyond lung protection by rescuing the suppressive effects of cigarette smoke on bone marrow hematopoietic progenitor cell function, and by restoring weight loss sustained by mice during cigarette smoke exposure. Pulmonary vascular protective effects of adipose stem cells were recapitulated by application of cell-free conditioned medium, which improved lung endothelial cell repair and recovery in a wound injury repair model and antagonized effects of cigarette smoke *in vitro*.

Conclusions: These results suggest a useful therapeutic effect of adipose stem cells on both lung and systemic injury induced by cigarette smoke, and implicate a lung vascular protective function of adipose stem cell derived paracrine factors.

Keywords: pulmonary disease, chronic obstructive; endothelium; cell death; regenerative medicine; human

Chronic obstructive pulmonary disease (COPD) including emphysema and chronic bronchitis is a prevalent condition primarily associated with cigarette smoking (CS). Patients affected by emphysema often exhibit progressive respiratory symptoms and loss of lung function, which in many culminates in respiratory failure, and systemic weight loss, which may lead

---

AT A GLANCE COMMENTARY

Scientific Knowledge on the Subject

Previous reports of encouraging lung protective and regenerative activities of both endothelial progenitor cells activated by the hepatocyte growth factor and autologous adipose stem cells (ASC) in the elastase-induced emphysema model prompted the current study of efficacy of ASC treatment in experimental cigarette smoke–induced emphysema. The effect of stem cell treatment on the systemic effects of cigarette smoking has not been previously explored.

What This Study Adds to the Field

This study shows that cigarette smoke–induced pulmonary emphysema in mice is attenuated by biweekly injections of ASC as evident by decreased inflammation, apoptosis, and alveolar enlargement induced by cigarette smoke *in vivo*. We document significant extrapulmonary effects induced by cigarette smoke in mice including the previously described weight loss, but also the less appreciated depression of bone marrow hematopoietic stem cell function. Most significantly, we describe that these *in vivo* extrapulmonary manifestations are markedly attenuated by treatment with ASC, suggesting an exciting therapeutic potential for both local and systemic injury in emphysema.

---

to cachexia. We and other research groups have shown that exaggerated (capillary endothelial cell) apoptosis, which may occur in the context of a vascular endothelial growth factor (VEGF)-deprived environment (1), is one contributing mechanism of lung injury in emphysema and an important therapeutic target (1–4). Because adult mesenchymal precursor/stem cells of adipose tissue origin protect against apoptosis of endothelial cells from systemic vascular beds (5, 6), we investigated the ability of these adipose-derived stromal (stem) cells (ASC) to inhibit the death of lung endothelial cells *in vivo* and limit the lung injury induced by CS.

There is increasing interest in exploiting the regenerative potential of stem cells for the treatment of lung diseases. Bone marrow (BM)-derived stem cells transplanted to the lungs can exhibit phenotypic and acquire functional markers of airway or alveolar epithelial cells, interstitial cells, and vascular endothelial cells (7). Potential lung protective and regenerative activities both of endothelial progenitor cells activated by the hepatocyte growth factor (HGF) and autologous ASC have been suggested in previous reports using an elastase-induced emphysema model (7, 8). Based on these findings, we sought to investigate in the context of a CS model the regenerative

potential of human or murine ASC. ASC constitute a distinct progenitor cell population within the adipose stromal compartment that has the practical advantage of an easily accessible and ethically uncontested source, being obtained in large numbers via liposuction from adults. The subcutaneous adipose tissue contains pluripotent cells in the stromal (nonadipose) compartment that can differentiate into multiple cell lineages, including neurons, skeletal myocytes, osteoblasts, chondroblasts, adipocytes, and vascular wall cells (9). Previous studies demonstrated that the protective properties of ASC are at least in part attributable to their capability to secrete multiple proangiogenic and antiapoptotic growth factors, including VEGF and HGF (10, 11), which act in a paracrine manner (11–14). In addition, ASC may directly partner with vascular endothelial cells to form vascular networks via a process of adult vasculogenesis (15). It is conceivable that ASC could home to regions of pulmonary endothelial injury and promote endothelial integrity both by secretion of antiapoptotic factors and by direct support of the pulmonary endothelium as mural cells. To test these hypotheses, we used two established experimental models of CS exposure– and VEGF receptor (VEGFR) blockade–induced emphysema, which share with human emphysema such characteristics as alveolar apoptosis, oxidative stress, and alveolar space enlargement and destruction (3, 16, 17). In addition to damaging pulmonary structures and function, long-term CS triggers clinically important extrapulmonary manifestations, including cardiovascular disease (18, 19), total body weight loss (20, 21), and decreased BM-derived stem cell differentiation and migration potential (22, 23). Although there has been significant progress in understanding the pathogenesis of and developing therapies for CS-induced cardiovascular dysfunction, much less is known about the mechanisms by which CS affects body mass and BM function, and no treatments exist for these conditions.

In the present study, intravenous administration of adult ASC of either human or mouse origin aimed at repairing the small vessel injury induced by CS or VEGFR inhibition improved both the pulmonary and systemic effects of CS in mice. These findings point the way to a new potential therapeutic option for COPD and other diseases involving disruption of the pulmonary architecture.

METHODS

Reagents and Antibodies

All chemical reagents were purchased from Sigma-Aldrich (St. Louis, MO), unless otherwise stated.

ASC Harvesting, Characterization, and Culture

Human ASC were isolated from human subcutaneous adipose tissue samples obtained from liposuction procedures, as previously described (24). Briefly, samples were digested in collagenase Type I solution (Worthington Biochemical, Lakewood, NJ) under agitation for 2 hours at 37°C, and centrifuged at 300 g for 8 minutes to separate the stromal cell fraction (pellet) from adipocytes. The pellets were filtered through 250 μm Nitex filters (Sefar America Inc., Kansas City, MO) and treated with red cell lysis buffer (154 mM NH_4Cl_2, 10 mM $KHCO_3$, and 0.1 mM ethylenediaminetetraacetic acid). The final pellet was resuspended and cultured in Endothelial Cell Growth Medium-2 (Lonza, Allendale, NJ). ASC were passaged when 60–80% confluent and used at passages three to six. Purity of ASC samples from endothelial cell contamination was confirmed by staining ASC monolayers with anti-CD31 antibodies. Mouse ASC were isolated in a similar fashion from adult DBA/2J, B6.129P2-$Apoe^{tm1\ Unc}$/J (Apo E), and B6;129S-Gt(ROSA)26Sor/J ("ROSA26") mice (25). ASC were labeled ex vivo, before intravenous administration, with DiI, a lipophilic carbocyanine that fluoresces after incorporation into cell membranes, using the

manufacturer's protocol (Invitrogen, Carlsbad, CA). Morbidity or mortality from embolic lodging of ASC administration was not seen unless the number of ASC injected exceeded 5×10^5, or the passage number of ASC expanded ex vivo exceeded three when a larger cellular size was noted, which prompted us to use mouse ASC up to passage three, followed by filtration through a 40-μM filter before injection.

Animal studies were approved by the Animal Care and Use Committee of Indiana University. C57Bl/6, Apo E, ROSA26, and DBA/2J mice were from Jackson Laboratories. At the end of the experiments, the mice were euthanized and the tissue was processed as described (3). In addition, mice underwent bronchoalveolar lavage (BAL), using phosphate-buffered saline (PBS) (0.6 ml). BAL cells were sedimented via centrifugation and counted after Giemsa staining of cytospins. The remaining acellular fluid was then snap-frozen in liquid nitrogen and stored at −80°C for further analysis.

In vivo CS exposure was performed as follows: C57Bl/6 (female; age 12 wk; n = 5–10 per group) or DBA/2J (male; age 12–14 wk; n = 5–10 per group) mice were exposed to CS or ambient air for up to 24 weeks. Briefly, mice were exposed to 11% mainstream and 89% side-stream smoke from reference cigarettes (3R4F; Tobacco Research Institute, KY) using a Teague 10E whole body exposure apparatus (Teague Enterprise, Woodland, CA). The exposure chamber atmosphere was monitored for total suspended particulates (average, 90 mg/m³) and carbon monoxide (average, 350 ppm). In all CS experiments, mice were euthanized and lungs were processed as previously described (3) the day after the last day of CS exposure.

VEGF receptor blockade was performed as previously described (3). NOD.Cg-Prkdc^scid $IL2R\gamma^{null}$ (NS2) mice (Indiana University Cancer Center Stem Cell Core) (female; age 9 wk) were injected with SU5416 (Calbiochem EMD, Gibbstown, NJ; 20 mg/kg, subcutaneously) or vehicle, carboxymethylcellulose, and the mice were euthanized at the indicated time.

Lung Disintegration and ASC Detection by Flow Cytometry

After euthanasia, the mouse trachea was cannulated and the thoracic cavity was opened. The lung vasculature was perfused with sterile PBS (20 ml; Invitrogen). The lung tissue was digested in 10% fetal bovine serum in Dulbecco's modified Eagle medium, 6.5 μg/ml DNase I, and 12 μg/ml collagenase I (Roche, Indianapolis, IN) (30 min; shaking 200 rpm; 37°C). The cell suspension was strained through a 70-μm cell strainer (Fisher Scientific, Fair Lawn, NJ) and cells were collected by centrifugation (500 × g; 5 min; 4°C). Cells were resuspended in Geyes solution, centrifuged as before, and collected in PBS, followed by fixation with paraformaldehyde (1%; 30 min; 21°C). Cells were then collected by centrifugation (500 × g; 5 min; 21°C), and resuspended in PBS for flow cytometry. Thirty thousand cells were analyzed for the presence of Vybrant DiI (Molecular Probes, Invitrogen) using flow cytometry (FC 500; emission 575 nm, excitation 488 nm).

Cell death was detected in inflated fixed lung sections, enabling specific evaluation of alveoli, rather than large airways and vessels (26), via active caspase-3 IHC (antibodies from Abcam and Cell Signaling, Cambridge, MA and Danvers, MA, respectively) (3), using rat serum as negative control. The immunostaining for active caspase-3 was followed by DAPI (Molecular Probes) nuclear counter-staining. Executioner caspase (caspase-3 or -7) activity was measured with ApoONE homogeneous Caspase-3/7 assay kit (Promega, Madison, WI) as described (3). Human recombinant caspase-3 (Calbiochem) was used as positive control.

Immunohistochemistry

Paraffin sections, or for some applications (green fluorescence protein [GFP] visualization) cryosections, were blocked with 10% rabbit (or goat serum, if secondary antibody from goat) and incubated with primary antibodies or control antibodies. Anti–caspase-3 (Cell Signaling) antibody was incubated for 1 hour at room temperature or at 4°C overnight. Bound antibody was detected according to the manufacturer's instructions using a biotin-conjugated goat anti-rat IgG secondary antibody (1:100; Vector Laboratories, Burlingame, CA) and streptavidin-coupled phycoerythrin or fluorescein isothiocyanate (1:1,000; Vector) were used. Sections were counterstained with DAPI and mounted with Mowiol 488 (Calbiochem). Microscopy was per-

formed on either a Nikon Eclipse (TE200S) inverted fluorescence or a combined confocal/multiphoton (Spectraphysics laser, BioRad MRC1024MP) inverted system. Images were captured in a masked fashion and quantitative intensity (expression) data were obtained by Metamorph Imaging software (Molecular Devices, Sunnyvale, CA) as previously described (4).

Morphometric analysis was performed in a masked fashion on coded slides as described, using a macro developed by Dr. Rubin M. Tuder (University of Colorado) for Metamorph (26, 27).

Lung volume measurements were performed with the flexiVent system (Scireq, Montreal, PQ, Canada). Mice were anesthetized with inhaled isoflurane in oxygen and orotracheally intubated with a 20-gauge intravenous cannula under direct vision. A good seal was confirmed by stable airway pressure during a sustained inflation. Isoflurane anesthesia was maintained throughout the measurements, and the mice were hyperventilated to eliminate spontaneous ventilation.

Western Blotting

Lung tissue was homogenized in Radio-Immunoprecipitation Assay buffer with protease inhibitors on ice and proteins were isolated by centrifugation at $16,000 \times g$ for 10 minutes at 4°C. Proteins were loaded in equal amounts (10–30 µg) as determined by bicinchoninic acid protein concentration assay (Pierce, Rockford, IL). Total proteins were separated by sodium dodecyl sulfate–polyacrylamide gel electrophoresis followed by immunoblotting. Primary antibodies were diluted in a sodium phosphate buffer containing 50 mM sodium phosphate, 150 mM NaCl, 0.05% Tween-20, 4% bovine serum albumin, and 1 mM sodium azide. Primary antibodies and their dilutions are as follows: ERK1/2 (1:2,000; Cell Signaling), phospho-ERK1/2 (1:1,000; Cell Signaling), p38 (1:1,000; Cell Signaling), phospho-p38 (1:1,000; Cell Signaling), JNK (1:1,000; Cell Signaling), phospho-JNK (1:1,000; Cell Signaling), vinculin (1:5,000; Calbiochem), or β-actin (1:30,000; Sigma). Blots were washed with TBS + 0.1% Tween-20 and incubated with HRP-conjugated secondary antibodies to rabbit (1:10,000; Amersham, Piscataway, NJ) or mouse (1:10,000; Amersham). Blots were detected using ECL-plus (Amersham) or SuperSignal (Pierce).

Hematopoietic Progenitor Cell Analysis

The absolute numbers and cell cycling status of granulocyte macrophage (colony forming unit– granulocyte, monocyte [CFU-GM]), erythroid (burst-forming unit–erythroid [BFU-E]), and multipotential (colony forming unit–granulocyte, erythrocyte, monocyte, and megakaryocyte [CFU-GEMM]) progenitor cells were calculated as previously reported (28, 29). In short, BM cells were flushed from femurs of control and treated mice, and nucleated cellularity calculated per femur. Femoral cells were treated *in vitro* with control medium, or high specific activity tritiated thymidine as a 30-minute pulse exposure, washed, and plated at 5×10^4 cells/ml in 1% methylcellulose culture medium with 30% fetal bovine serum (Hyclone, Logan, UT), and recombinant human erythropoietin (Epo, 1 U/ml, Amgen Corp, Thousand Oaks, CA), recombinant murine stem cell factor (50 ng/ml, R&D Systems, Minneapolis, MN), and 5% vol/vol pokeweed mitogen mouse spleen cell conditioned medium (29). Semisolid cell cultures were placed in culture at 5% CO_2 at lowered (5%) O_2 in a humidified chamber, and CFU-GM, BFU-E, and CFU-GEMM colonies scored after 7 days incubation. The number of colonies and femoral nucleated cellularity was used to calculate numbers of progenitors per femur. The high specific activity tritiated thymidine kill assay allows an estimate of the cell cycling status of progenitors by analysis of the percent progenitors in S-phase at time cells were removed from mice and plated (29).

Lung Endothelial Cells

Primary human lung microvascular endothelial cells were obtained from Lonza and maintained in culture medium consisting of Endothelial Basal Medium-2, 5% fetal bovine serum, 0.4% hydrocortisone, 1.6% human fibroblast growth factor (hFGF), 1% VEGF, 1% insulin-like growth factor-1, 1% ascorbic acid, 1% human epidermal growth factor, 1% gentamicin-amphotericin-B, and 1% heparin at 37°C in 5% CO_2 and 95% air. Experiments were performed up to passage 10 with cells at 80–100% confluence.

CS Extract Preparation

An aqueous CS extract was prepared from filtered research-grade cigarettes (1R3F) from the Kentucky Tobacco Research and Development Center at the University of Kentucky. A stock (100%) CS extract was prepared by bubbling smoke from two cigarettes into 20 ml of basal culture medium (EBM2; Lonza) at a rate of one cigarette per minute to 0.5 cm above the filter, using a modified method developed by Carp and Janoff (30). The extract's pH was adjusted to 7.4, followed by filtration (0.2 µm, 25 mm Acrodisc; Pall, Ann Arbor, MI) and used in cell culture experiments within 20 minutes. A similar procedure was used to prepare the control extract, replacing the CS with ambient air.

Endothelial Cell Wound Repair Assays

Wounding of cultured cells was performed using the Electric Cell Impedance System (ECIS, Applied Biophysics, Troy, NY). Human lung microvascular endothelial cells were grown as detailed previously on gold microelectrodes (8W1E) until confluent. Cells were pretreated for 2 hours in basal medium or in conditioned medium collected from cultured adult human ASC (50% vol/vol). Cells were then treated wounded via a linear electrical injury applied via ECIS, in the presence or absence of CS extract (4%). Wound repair was quantified by measuring cellular resistance over time and normalizing it to the time of wounding, reporting the slope of the transendothelial electrical resistance (TER) recovery until monolayer confluence was achieved.

Statistical Analysis

Statistical analysis was performed with SigmaStat software using analysis of variance with Student-Newman-Keuls *post hoc* test, or Student t test. Statistical difference was accepted at P less than 0.05.

RESULTS

ASC Characterization and Localization in the Lungs after Systemic Delivery

Initial studies of the distribution of ASC after systemic administration were conducted using ROSA26 mouse-derived ASC expressing β-galactosidase under the control of an unknown endogenous promoter delivered intravenously into non–β-galactosidase expressing mice bearing a homozygous deletion of the Apo E locus. Tissues of these animals were stained for β-galactosidase expression at 1, 7, and 21 days after delivery. Gross inspection 1 hour after administration revealed a predominantly pulmonary localization, with a pattern of distribution consistent with intravascular trapping (*see* Figure E1A in the online supplement), which was confirmed histologically by the presence of ASC in the lung parenchyma in lacZ-ASC–treated wild-type mice, which exhibited X-gal staining, compared with vehicle-injected control wild-type mice, which lacked X-gal staining (Figure 1A). Interestingly, evaluation at 7 and 21 days after ASC delivery demonstrated focal areas of staining consistent with incorporation of lacZ–expressing cells in the airway epithelium, including that of medium and large-sized airways (Figure 1A).

In separate homing experiments, autologous GFP-labeled mouse ASC (3×10^5 cells) were administered systemically via intravenous injection to DBA/2J mice. Using immunohistochemistry, GFP-labeled cells were detected in the lung alongside resident cells in both large airway epithelial and subepithelial structures (*see* Figure E1B), and in parenchymal, vascular and alveolar structures at 1 week after their administration (*see* Figure E1C). To avoid potential immunostaining artifacts and interference with the lung autofluorescence, and to allow for a more quantitative assessment, Vybrant DiI-labeled autologous ASC were injected into DBA/2J mice followed by
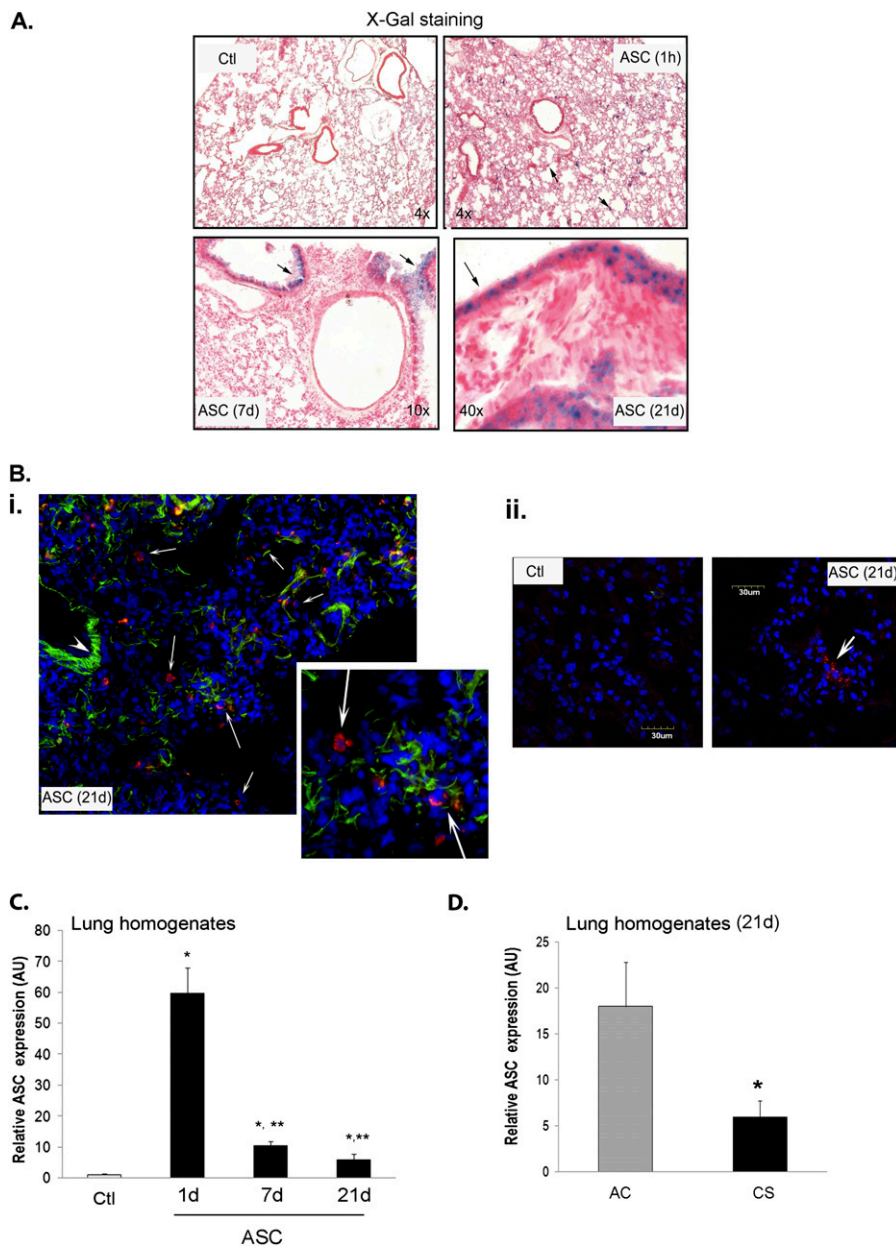
Figure 1. Lung homing of adult adipose stem cells (ASC) delivered by intravenous administration to mice. (A) Localization of B-galactosidase–expressing murine ASC (blue) on lung sections imaged at the indicated magnification after fixation and staining with X-Gal and hematoxylin. Lungs of Apo E mice were harvested at the indicated time (1 h, 7 and 21 d) after 5×10^5 ASC or control vehicle (Ctl) administration. Note (arrows) the presence of ASC in the lung parenchyma (1 h) and among the bronchial epithelial layer (7 and 21 d). (B) Epifluorescence (i; inset) and confocal fluorescence (ii) micrographs of frozen-sectioned lungs from DBA/2J mice harvested 21 days after a single injection with DiI-labeled ASC (3×10^5) or vehicle (controls) and stained with DAPI (blue). Note perinuclear red fluorescence (arrows) in the ASC-injected mice, and green autofluorescence of elastin structures in the lung (arrowhead in i). (C) Abundance of DiI-labeled murine ASC detected by flow cytometry of whole-lung homogenates obtained by digestion and disintegration. Lungs were harvested 1, 7, and 21 days after ASC administration (3×10^5) or vehicle in DBA/2J mice previously exposed to cigarette smoking for 2 weeks. All ASC groups *$P < 0.05$ versus vehicle control; **$P < 0.05$ versus day 1; n = 4–5; analysis of variance. (D) Abundance of cell events consistent with DiI-labeled murine ASC detected by flow cytometry of lung homogenates harvested 21 days after a single ASC administration (3×10^5) or vehicle in DBA/2J mice previously exposed to cigarette smoking (CS) or air control (AC) for 2 weeks. Mean + SEM; *$P < 0.05$ versus AC; n = 4–5.

immunofluorescence microscopy on frozen lung sections at Day 21 (Figure 1B) and the persistence of the labeled ASC was evaluated by flow cytometry of disintegrated lungs at Days 1, 7, and 21 after a single injection of ASC (Figures 1C and 1D). DiI-labeled ASC were detected at 21 days using epifluorescence and confocal fluorescence microscopy in the lung parenchyma of ASC-injected mice, but not littermate mice injected with vehicle (Figure 1B). In contrast, evaluation of the BM of mice exposed to either ambient air or CS at 21 days after a single intravenous injection of DiI-labeled ASC revealed no significant trapping of ASC (data not shown). Consistent with our experience of initial retention of mouse ASC in the lung after systemic delivery in Apo E mice, the injected DiI-labeled mouse ASC were found in significantly higher numbers in the lungs at Day 1, compared with 7 or 21 days after injection ($P < 0.05$). Interestingly, exposure to CS for 2 weeks before ASC injection led to a decrease in lung trapping of ASC at 21 days (Figure 1D). It is not known whether the persistence of ASC in the lungs is required for their putative regenerative effects in

the lung. Given this uncertainty, we next investigated whether repetitive injection of ASC was sufficient to prevent airspace enlargement in CS-induced emphysema, the disease model of highest clinical relevance. To ensure that all expected components of the emphysematous process including inflammatory elements remained intact, for these studies we elected to use DBA/2J mice with isogenic mouse-derived ASC.

Treatment with ASC Decreased CS-induced Lung Inflammation, Caspase Activation, and Airspace Enlargement

DBA/2J mice were exposed to CS or ambient air for 4 months, whereas a third group of mice, also exposed to CS in parallel, were given ASC collected from littermate mice, expanded ex vivo, and administered by intravenous injection every other week during the last 2 months of the 4-month CS exposure. In a second similar experiment, a fourth group of CS-exposed mice received ASC carrier as a vehicle control. As expected, CS

exposure (4 mo) in the DBA/2J mice increased lung inflammation, measured by an elevated number of inflammatory cells (macrophages and polymorphonuclear cells) in the BAL (Figures 2A and 2B), increased alveolar cell death, measured by caspase-3 activity and immunohistochemistry (Figures 2C–2E), and caused significant alveolar space enlargement, measured by the standardized automated morphometry of alveolar structures on hematoxylin and eosin–stained lung sections, when compared with control animals exposed to ambient air (Figure 3). In the group receiving systemic injections of ASC, there was an attenuation of the CS-induced increase in the number of macrophages and polymorphonuclear leukocytes in the BAL (Figures 2A and 2B). ASC treatment attenuated the enzymatic activity of caspase-3 in total lung homogenates by more than 30% ($P = 0.02$) (Figure 2C), and markedly decreased the CS-induced active caspase-3 expression in the lung parenchyma, measured by immunohistochemistry (Figures 2D and 2E) when compared with the CS-exposed mice who did not receive ASC or who only received vehicle control. These protective effects were associated with a significant decrease in alveolar space size

compared with the group exposed to CS alone (Figure 3A). This was reflected by a significant decrease in the mean linear intercepts from to 40.5 $\pm$ 1 to 36.3 $\pm$ 0.7 μm ($P = 0.01$), a significant increase in alveolar surface area from 115.7 $\pm$ 36 to 280.1 $\pm$ 34 mm^2 ($P = 0.004$) (Figure 3B), and a significant attenuation of lung volume enlargement ($P = 0.01$) (Figure 3C). The protective effects of ASC on lung inflammation, caspase activation, and alveolar integrity were associated with biochemical evidence of modulation of the CS-induced MAPK signal transduction pathways involved in inflammation and apoptosis. Treatment with ASC abrogated the phosphorylation of p38 MAPK and attenuated JNK1 and AKT activities induced by the chronic CS exposure (*see* Figure E2).

Treatment with ASC Prevented CS-induced Weight Loss in Mice

As previously noted (20), chronic CS exposure caused a significant decrease in body weight, reaching 10% after 4 months of exposure ($P = 0.003$) compared with mice of similar age and sex exposed to ambient air for the same duration of time (Figure 4A).
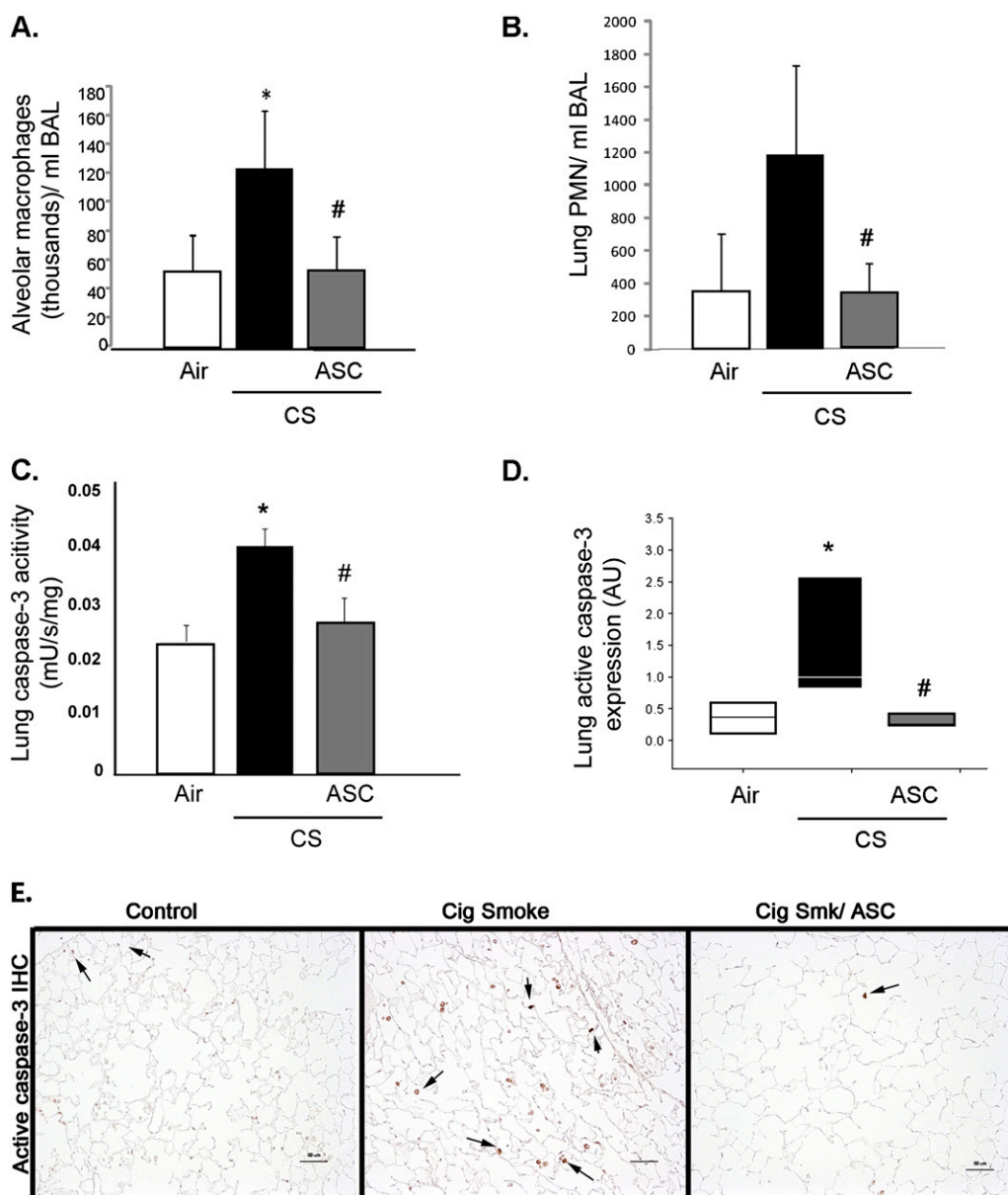

Figure 2. Effect of adipose stem cells (ASC) treatment on cigarette smoking (CS)–induced inflammation and caspase activation. Abundance of inflammatory cells alveolar macrophages (*A*) and polymorphonuclear cells (*B*) in the bronchoalveolar lavage (BAL) fluid collected from DBA/2J mice exposed to CS or ambient air (Air) for 4 months (n = 8–12 per group) and treated with ASCs (3×10^5 cells infused intravenously every other week, during mo 3 and 4 of CS exposure). *$P <$ 0.05 versus control; #$P <$ 0.05 versus CS; analysis of variance (ANOVA). Lung cell death was quantified in the same experiment by caspase-3 activity measured with a fluorimetric enzymatic kinetic assay and normalized by protein concentration in lung homogenates (*C*; mean + SEM; *$P <$ 0.05 vs. vehicle control; ANOVA) and by abundance of active caspase-3-expressing cells in lung parenchyma measured (*D*; median box plot; arbitrary units [AU]; *$P <$ 0.05 vs. air control; #$P <$ 0.05 vs. CS; ANOVA) by automated image analysis of lung sections immunostained with a specific antibody (*E*). Note active caspase-3 expressing cells in the alveolar tissue (*arrows*).
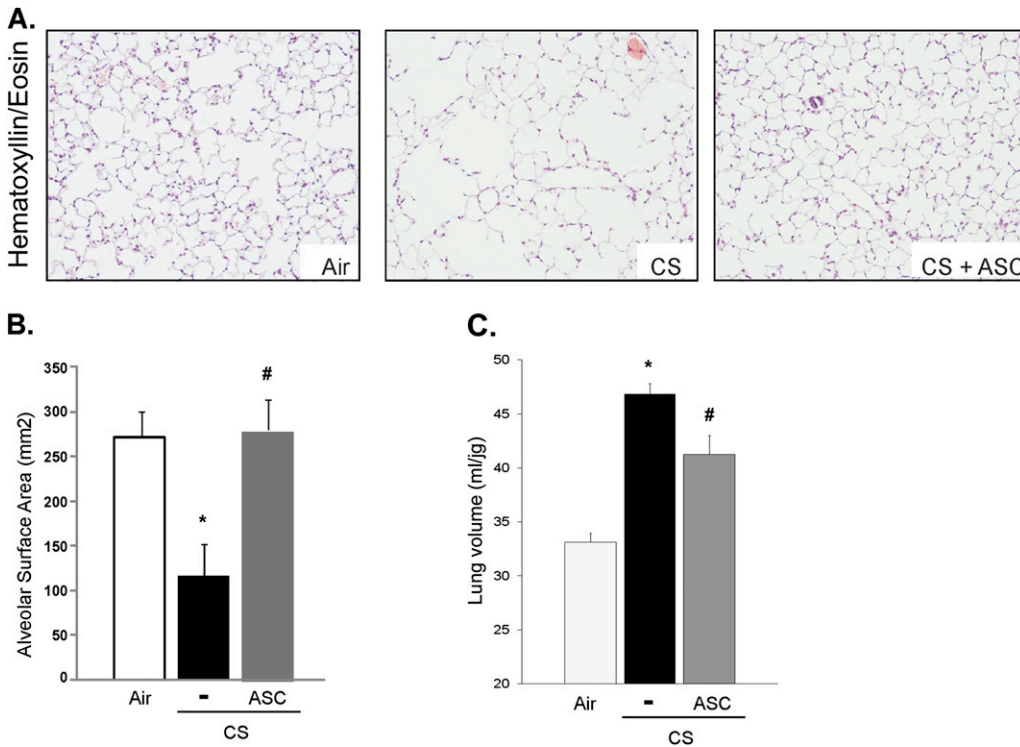
Figure 3. Effect of adipose stem cells (ASC) treatment on cigarette smoking (CS)–induced airspace enlargement. (*A*) Alveolar airspaces stained with hematoxylin and eosin on fixed lung sections from mice exposed to CS or ambient air for 4 months. DBA/2J mice were treated with ASC (3×10^5 cells per injection, injected intravenously every other week), during months 3 and 4 of CS exposure. Note the increased airspaces in the CS-exposed mice and the smaller airspaces in the CS-exposed mice treated with ASC. (*B*) Alveolar surface area calculated by standardized morphometry of alveolar spaces on coded slides (mean + SEM; *$P <$ 0.05 vs. air control; #$P <$ 0.05 vs. CS; analysis of variance). (*C*) Lung volumes measured in anesthetized and intubated DBA/2J mice (n = 5–10) at 4 months after CS exposure (mean + SEM; *$P <$ 0.05 vs. air control; #$P <$ 0.05 vs. CS; analysis of variance).

Interestingly, CS-exposed mice treated with ASC during the last 2 months of exposure had no significant weight loss compared with ambient air–exposed control animals (Figure 4A; *see* Figure E3). When examined macroscopically, the area of fat measured from coded (masked) photographs of the abdominal subcutaneous region, the ASC-treated mice had a significant increase ($P <$ 0.05) in the abundance of subcutaneous fat compared with the untreated CS-exposed mice, (Figures 4B and 4C). Macroscopically, no difference in the body distribution of fat was noted compared with that in control mice (data not shown).

Treatment with ASC Restored the BM Dysfunction Induced by CS in Adult Mice

One of the less widely appreciated and studied systemic effects of CS exposure is the suppression of BM function (31, 32). To evaluate the capability of ASC to modulate the toxic effects of chronic CS exposure on hematopoiesis, BM was harvested from
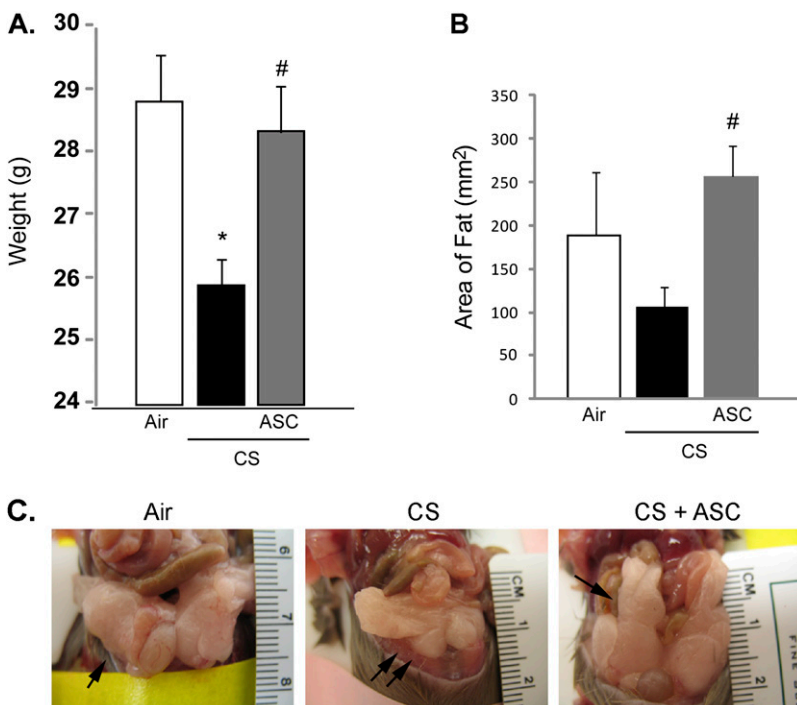

Figure 4. Effect of adipose stem cells (ASC) treatment on cigarette smoking (CS)–induced weight loss in mice. (*A*) Body weight of DBA/2J mice after 4 months of air or CS exposure. A third group was treated with ASC (3×10^5 cells per injection, injected intravenously every other week), during months 3 and 4 of CS exposure (mean +SEM; n = 10–12; *$P <$ 0.05 vs. air control; #$P <$ 0.05 vs. CS; analysis of variance). (*B*) Abundance of abdominal fat (mean + SEM; n = 3–6; #$P <$ 0.05 vs. CS; analysis of variance), measured at 4 months. (*C*). Note the marked decrease in the amount of abdominal fat in the CS-exposed mice (*double arrows*), compared with control mice and with ASC-treated CS-exposed mice (*arrows*).

the femora of DBA/2J mice exposed to CS for 4 months that received either control carrier or ASC. CS exposure resulted in a marked and significant reduction in absolute numbers of BM CFU-GM, BFU-E, and CFU-GEMM, with these progenitors being in a slow or noncycling state. In stark contrast, ASC treatment during the last 2 months of CS exposure fully or nearly completely counteracted the suppressive effects of CS on BM function (Figures 5A–5D).

Treatment with Human ASC Decreased VEGFR Inhibitor–induced Airspace Enlargement in Immunodeficient mice

The mechanisms by which ASC exerted their protective local and systemic effects in the CS model may include paracrine release of survival and growth factors, including VEGF (33, 34), which oppose the excessive apoptosis noted in response to CS exposure. To address this hypothesis, we next used a complementary model of emphysema driven by apoptosis caused by decreased VEGF availability. We have previously demonstrated that VEGFR blockade with SU5416 (20 mg/kg, subcutaneously) caused significant increases in airspace enlargement in C57Bl/6 mice that peaked at 28 days (3). This airspace enlargement is dependent on alveolar cell apoptosis (1, 3), detected not only in endothelial but also in epithelial cell types (3), making this model ideally suited to address whether ASC treatment is sufficient to overcome a VEGF-deprived state and influence endothelial survival. In addition, to investigate whether

not only the mouse, but also the human adult ASC are efficient at protecting against lung apoptosis, we used immunodeficient Nod-SCID IL-2 receptor γ chain-deficient (NS2) mice. Pilot experiments using this mouse demonstrated that the immuno-tolerant NS2 mouse is susceptible to development of airspace enlargement as a result of VEGFR blockade. Indeed, administration of SU5416 (20 mg/kg, subcutaneously) showed the NS2 mice exhibited a significant increase in alveolar enlargement at 21 days compared with vehicle (carboxymethylcellulose) controls in both male and female adult mice (data not shown).

Because systemically delivered ASC preferentially lodge and engraft in the lungs of mice 24 hours after systemic delivery, we administered human ASC (3×10^5 cells, intravenous injection) at Day 3 after VEGFR inhibition in adult NS2 female mice, a time at which lung apoptosis is increasing in this model, peaking between 3 and 7 days of VEGFR administration (3). GFP-labeled human ASC were detected in the lungs of NS2 mice 3 days after injection (Day 6 of VEGFR blockade), as determined by GFP immunoblotting of total lung homogenates (*see* Figure E1B). At 28 days, the VEGFR blockade-induced increase in cell death, measured by image analysis and quantification of the immunohistochemical expression of active caspase-3 in the lung parenchyma, was significantly attenuated by 75% ($P = 0.03$) after treatment with a single injection of human adult ASC (Figures 6A and 6B). Furthermore, the VEGFR-blockade–induced alveolar enlargement was significantly decreased, measured by a 70% improvement ($P = 0.006$) in mean
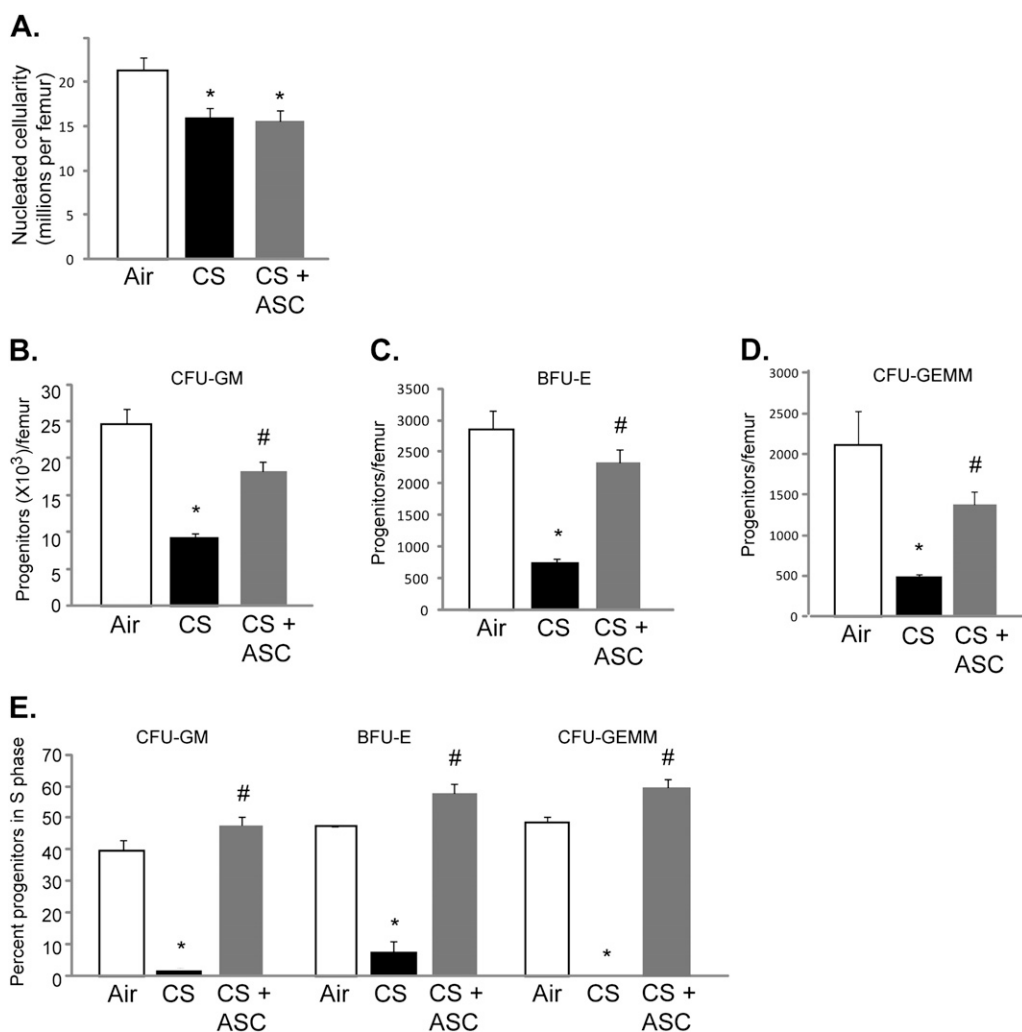

Figure 5. Effect of adipose stem cells (ASC) treatment on cigarette smoking (CS)–induced bone marrow (BM) dysfunction in mice. Absolute numbers of nucleated cells (*A*) and hematopoietic progenitors colony forming unit-granulocyte, monocyte (CFU-GM) (*B*), burst-forming unit-erythroid (BFU-E) (*C*), colony forming unit-granulocyte, erythrocyte, monocyte, and megakaryocyte, CFU-GEMM (*D*), and cycling status (= percent cells in S-phase) of these progenitors (*E*) in DBA/2J mice after 4 months of air or CS exposure, with a third group treated with ASC (3×10^5 cells per injection, injected intravenously every other week), during months 3 and 4 of CS exposure (mean + SEM; n = 4–6; *$P < 0.05$ vs. air control; #$P < 0.005$ vs. CS; analysis of variance).
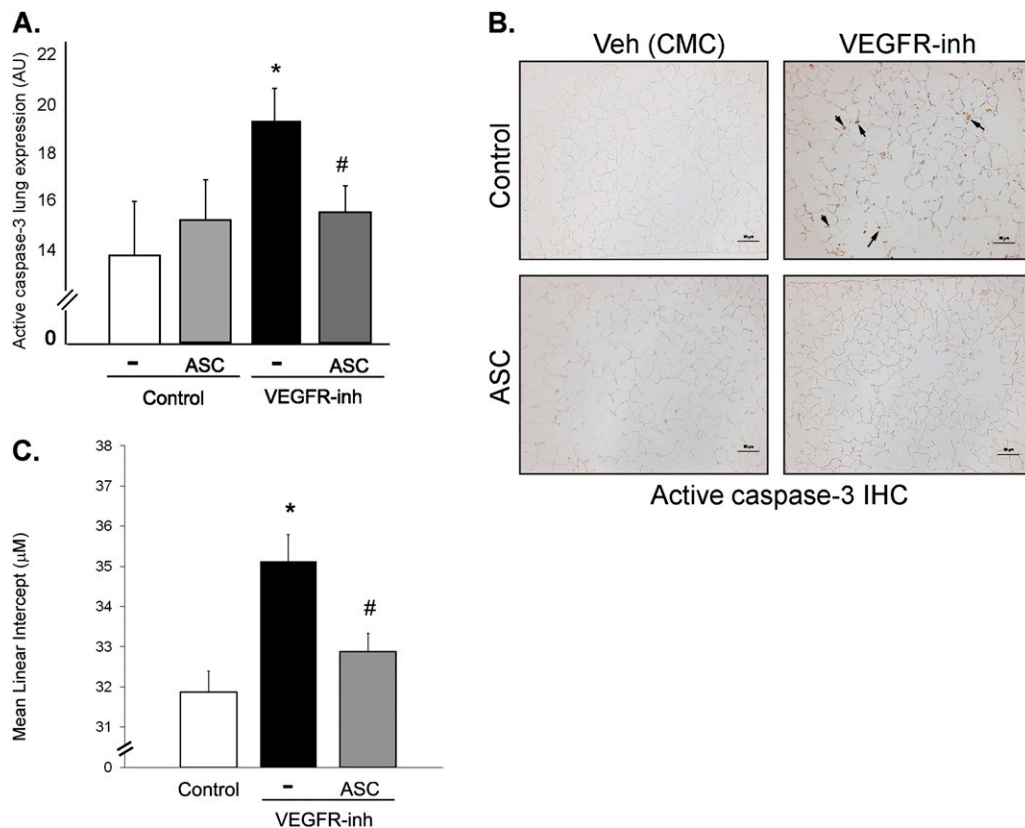
Figure 6. Adipose stem cells (ASC) efficacy in an apoptosis–dependent alveolar enlargement model. (*A, B*) Lung cell death was quantified by abundance of active caspase-3 expressing cells in lung parenchyma (at 4 wk) in animals (Nod-SCID NS2 mice) who received a single dose of vascular endothelial growth factor receptor (VEGFR) inhibitor (SU5416, 20 mg/kg; sq) or its vehicle control (carboxymethylcellulose), and who were treated with human adult ASC (3×10^5, intravenous injection) on Day 3 after VEGFR inhibition; (*A*; mean arbitrary units (AU) + SEM; *$P < 0.05$ vs. vehicle [*control*]; #$P < 0.05$ vs. ASC-untreated [-] animals who received the VEGFR-inhibitor; analysis of variance). Quantification was achieved by image analysis of lung sections immunostained with a specific active caspase-3 antibody (*B*; *brown*; *arrows*). (*C*) Mean linear intercepts calculated by standardized morphometry of alveolar spaces stained with hematoxylin and eosin from mice exposed to carboxymethylcellulose vehicle or VEGFR-inhibitor for 24 weeks and treated with ASC as above (mean + SEM; *$P < 0.05$ vs. vehicle control; #$P < 0.05$ vs. VEGFR-inhibited mice; analysis of variance).

linear intercepts after the systemic administration of human adult ASC (Figure 6C). These results suggested ASC have prominent protective antiapoptotic effects in the lung, overcoming the specific effects of VEGF inhibition.

Human ASC-Conditioned Medium Improved the Repair of Lung Endothelial Cell Monolayers *In Vitro*

To determine whether ASC are capable of providing a protective effect toward injured lung microvascular endothelial cells specifically via a paracrine mechanism, we studied adult human ASC-conditioned medium (ASC-CM) in an *in vitro* model of lung endothelial injury. The integrity of the normally tight cultured lung endothelial cell monolayers can be tracked in real time by measuring the TER of cells grown on microelectrodes, using ECIS. Using this approach, we studied the effect of ASC-CM on lung endothelial cell wound repair after wounding induced by a linear electrical injury applied through microelectrodes in contact with the monolayer. After wounding, which is characterized by a sudden decrease in TER, the monolayer repairs via both cell growth and migration of endothelial cells from the wound edges toward the "wound" (35), which is reflected by a gradual restoration of TER toward that of confluent monolayers. Cell monolayers grown at confluence were "wounded" via a linear electrical injury applied through microelectrodes in contact with the monolayer. Pretreatment of primary human lung microvascular endothelial cell monolayers with ASC-CM significantly ($P = 0.003$) enhanced the TER recovery after wounding compared with untreated cells (Figures 7A and 7B). Interestingly, in the presence of a CS extract, which contains a water-soluble fraction of CS that mimics its circulating components, there was a marked delay in

lung endothelial cell wound healing (Figures 7A and 7C); both the slope of TER recovery and the absolute TER attained at full recovery after wounding were significantly blunted compared with wounded endothelial cells exposed to ambient air-extract control. Strikingly, endothelial cell monolayers repaired the wound significantly faster in the presence of ASC-CM, even during concomitant CS extract exposure (Figure 7A). Because the ASC-CM contains serum necessary for their growth, and because serum itself has numerous growth factors, we investigated the effect of the control-conditioned medium, which contained serum on wound repair. Although serum exerted a marked protective effect on the slope of wound repair, only cells treated with ASC-CM sustained their monolayer barrier function attained after wounding (Figures 7B and 7C). These data suggest that factors secreted by ASC exert protective effects against lung endothelial cell damage and may antagonize the injurious effects of CS exposure.

DISCUSSION

These results demonstrate that both murine and human ASC are capable of significantly ameliorating the pulmonary damage caused by CS exposure, even when administered mid-way during a temporally protracted CS exposure. The observed profound protective effects of ASC in the murine lung, and the vascular protective properties of paracrine factors secreted by these cells, render such therapy a potentially promising intervention in emphysema. Recognition of the importance of endothelial apoptosis in experimental pulmonary emphysema (1, 3, 4), including after tobacco smoke exposure (36, 37), has prompted a focus on the potential role for vascular cell–responsive growth factor modulation as a novel approach to
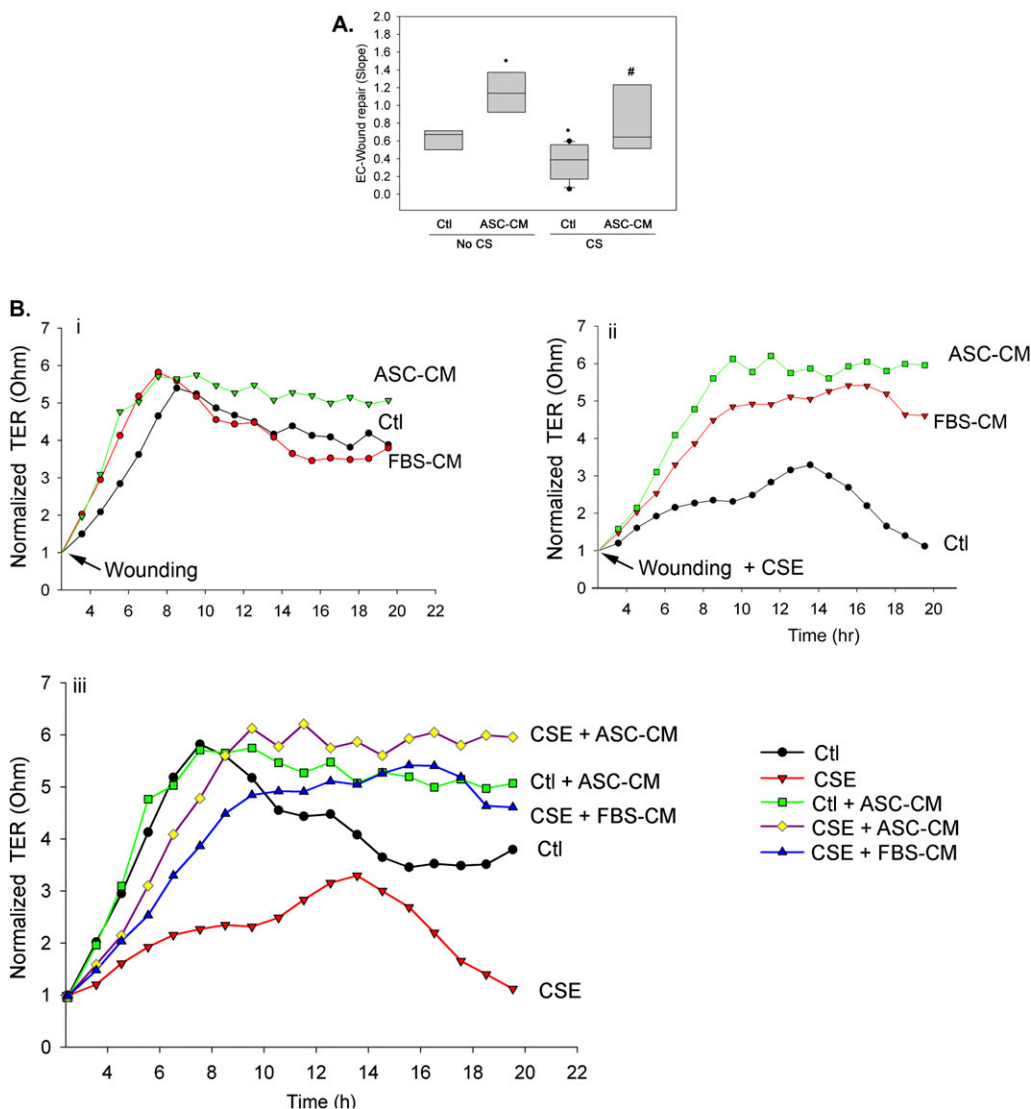
Figure 7. Paracrine effects of adipose stem cells (ASC) on lung endothelia injury *in vitro*. (*A–C*) Wound injury repair measured by the recovery of transcellular electrical resistance (TER) across a confluent monolayer of primary human lung microvascular endothelial cells grown on gold microelectrodes using the Electric Cell-Substrate Impedance Sensing system. A linear electrical injury was applied at time 2.4 hours (*B*, *C*, arrow) and the slope of TER recovery to plateau was compared for cells maintained in their regular growth medium, or in medium supplemented with conditioned medium from ASC cells (ASC-CM; 50%), in the absence and presence of cigarette smoking (CS) extract (4%). (*A*) Box plot with medians; n = 4 independent experiments; $P < 0.01$ two-way analysis of variance for the effect of CS and ASC-CM; *$P < 0.005$ versus untreated wounded control cells; #$P < 0.005$ versus untreated wounded CS-exposed cells. (*B*) Kinetics of normalized TER (to the TER at time of wound application) (mean; n = 3–4 independent experiments) in unexposed cells (*i*) or in cells exposed to CS (*ii*) wounded at time 2.4 hours (*arrow*), which were either untreated, grown in their control medium (*Ctl*; *black line*), or treated with ASC-CM (*green line*) or with control serum-containing media (fetal bovine serum [FBS]-CM, 20%; *red line*). Note the effect of CS extract on both the slope and the attained plateau levels of TER recovery in wounded lung endothelial cells and the protective effects of both ASC-CM and serum on the slope of TER recovery, with ASC-CM-specific effects on the plateau TER, evident in panel (*iii*), which combines conditions shown in panels *i* and *ii*.

treatment. Models involving endothelial apoptosis caused by either exposure to CS or specific impairment of endothelial survival by VEGFR-blockade allow the evaluation of putative therapies in the context of a clinically relevant toxic exposure and a specific molecular lesion, respectively. Our previous demonstration that ASC can elicit both angiogenic and anti-apoptotic effects in multiple systems (5, 6, 14) led us to hypothesize that the systemic administration of ASC may help to restore damaged pulmonary capillary networks and also may serve to protect the alveolar architecture from destruction in these models of emphysema. Prior studies have shown that both intravenous systemic administration of ASC and local placement of ASC on a synthetic scaffold could limit the extent of elastase-induced emphysema and accelerate lung growth after experimental lung volume reduction surgery in rats (38–40), but have not investigated their activity in the context of CS exposure.

The therapeutic effects of ASC on the pulmonary system may engage multiple mechanisms, including secretion of anti-apoptotic factors with paracrine protective action on neighboring resident lung cells, activation of endogenous progenitor cell cycling and differentiation, rescue and recruitment of circulating cells engaged in pulmonary repair, and direct differentiation into pulmonary epithelial or endothelial cells. The relatively low number of ASC detectable in lung tissue several days after administration, coupled with their effective antiapoptotic and overall lung protective effects, suggest that an important therapeutic function of ASC may be to promote endogenous repair processes and limit damage through paracrine effects. Similar protective effects of ASC delivery in the VEGF-inhibition model of emphysema support the notion that VEGF is one of the factors secreted by ASC, which exert protective effects on lung endothelial cells, much as we have described previously in the context of cultured endothelial cells (10). Although the paracrine effects of ASC on cultured lung endothelium are corroborative, they cannot be directly extrapolated to complex animal models of CS-induced emphysema and therefore more studies are needed to define the extent to which these paracrine effects may occur *in vivo*. Such paracrine effects may be combined with a direct cellular integration of ASC among other structural components of the lung, a scenario suggested by the detection of ASC for up to 3 weeks after

injection, intercalated among alveolar cells in the parenchyma and among epithelial cells in large airways. Although the relevance of this integration is not yet established, it is possible that ASC may be directly participating in tissue regeneration to limit CS-induced lung injury.

Our data revealed a novel function of adult ASC in promoting the repair of the lung endothelial barrier function, even in the presence of CS. These vascular protective properties of ASC are in agreement with previous reports of BM-derived progenitor stem cells that can reduce lung vascular permeability (41) and may be explained by their endogenous localization in the adipose tissue in a perivascular niche, where they exhibit prepericytes markers (24). Furthermore, ASC secrete potent prosurvival factors and ASC-CM has exerted antiapoptotic effects on systemic vascular endothelial cells, which has been shown to be predominantly mediated through the actions HGF and VEGF on angiogenesis and the formation of new vessels (33).

Remarkably, the marked effects of chronic CS exposure on body weight, adipose depots, and hematopoietic progenitor cycling and colony formation of multiple BM colony-forming types were substantially reversed by ASC, demonstrating that the provision of ASC results in systemic protection against diverse pathologies induced by such smoke exposure. Substantial weight loss in the context of CS is a well-known clinical phenomenon and described previously in C57Bl/6 mice exposed to CS for 9 weeks (20, 21). We noted a similar effect of CS in the DBA/2J mice. The weight loss (cachexia) associated with advanced stages of COPD portends a poor prognosis for these patients, even after smoking cessation, and has no effective treatment. Therefore, the ability of the ASC to reverse the weight loss may be of great therapeutic promise, although the mechanisms of action and the cell-type specificity of this effect remain to be determined. It is interesting that such cachexia may be the result of excessive circulating tumor necrosis factor-α levels (42). In fact, a recent study of BM-derived mesenchymal stem cells, which bear substantial similarity to ASC (43, 44), demonstrated that BM mesenchymal stem cells, which also predominantly localized in the lung after intravenous administration, promote systemic tissue repair by secreting several specific molecules in response to elevated levels of circulating tumor necrosis factor-α found in the context of tissue damage (45). It is intriguing to speculate that such a tumor necrosis factor-α–mediated activation of ASC may likewise induce secretion of a spectrum of molecules that block the cachectic effects of tumor necrosis factor-α.

The BM is the main adult repository for hematopoietic stem cells and an important source for endothelial progenitors; and each of these populations has been reported to be depressed because of CS or nicotine, a major component of CS (22, 23, 32). In addition, reports by Liu and coworkers (31), among others, have noted that CS causes the release of immature eosinophils from BM and that Balb/c mice exposed to nicotine demonstrate impairment of hematopoetic stem cell migration, which is hypothesized to alter stem cell homing (32, 46). Further in vitro data have demonstrated that CS extract strikingly diminishes BM progenitor cell chemotaxis in Boyden chamber assays. Our analysis of the BM from mice exposed to CS revealed that BM-derived progenitor cells had diminished proliferation capacity and were decreased in number. It remains to be shown whether these progenitor cells might be mediators of ASC-induced lung protection and whether their inhibition caused by CS exposure could contribute to an inability to repair the lung parenchyma in COPD. Should that be the case, ASC-induced restoration of BM progenitor cell cycling and numbers might constitute a novel mechanism by which these cells exert as well as pulmonary vascular protective effects. The mecha-

nism by which administration of ASC restored the proliferation of the hematopoietic progenitor cells remains unknown, but could potentially involve molecules that overlap with those active in sustaining body mass as described previously. Identification of these mechanisms will be helpful both in defining approaches to ASC therapeutic use and for potentially pointing the way to new molecular targets for therapeutic intervention in pulmonary emphysema.

Conclusions

Adult ASC exert protective properties against lung endothelial injury and against pulmonary and systemic deleterious effects of CS exposure, including airspace enlargement, weight loss, and BM suppression. These cells, which are a readily available population of highly proliferative and clonogenic cells resident in the stromal fraction of adipose tissues and may be readily expanded in vitro, may represent a potential therapeutic option in lung diseases characterized by excessive apoptosis, including pulmonary emphysema.

References

1. Kasahara Y, Tuder RM, Taraseviciene-Stewart L, Le Cras TD, Abman S, Hirth PK, Waltenberger J, Voelkel NF. Inhibition of VEGF receptors causes lung cell apoptosis and emphysema. *J Clin Invest* 2000;106:1311–1319.
2. Diab KJ, Adamowicz JJ, Kamocki K, Rush NI, Garrison J, Gu Y, Schweitzer KS, Skobeleva A, Rajashekhar G, Hubbard WC, *et al.* Stimulation of sphingosine 1 phosphate signaling as an alveolar cell survival strategy in emphysema. *Am J Respir Crit Care Med* 2010;181: 344–352.
3. Petrache I, Natarajan V, Zhen L, Medler TR, Richter AT, Cho C, Hubbard WC, Berdyshev EV, Tuder RM. Ceramide upregulation causes pulmonary cell apoptosis and emphysema-like disease in mice. *Nat Med* 2005;11:491–498.
4. Giordano RJ, Lahdenranta J, Zhen L, Chukwueke U, Petrache I, Langley RR, Fidler IJ, Pasqualini R, Tuder RM, Arap W. Targeted induction of lung endothelial cell apoptosis causes emphysema-like changes in the mouse. *J Biol Chem* 2008;283:29447–29460.
5. Cai L, Johnstone BH, Cook TG, Liang Z, Traktuev D, Cornetta K, Ingram DA, Rosen ED, March KL. Suppression of hepatocyte growth factor production impairs the ability of adipose-derived stem cells to promote ischemic tissue revascularization. *Stem Cells* 2007;25: 3234–3243.
6. Wei X, Du Z, Zhao L, Feng D, Wei G, He Y, Tan J, Lee WH, Hampel H, Dodel R, *et al.* Ifats collection: the conditioned media of adipose stromal cells protect against hypoxia-ischemia-induced brain damage in neonatal rats. *Stem Cells* 2009;27:478–488.
7. Ishizawa K, Kubo H, Yamada M, Kobayashi S, Numasaki M, Ueda S, Suzuki T, Sasaki H. Bone marrow-derived cells contribute to lung

regeneration after elastase-induced pulmonary emphysema. *FEBS Lett* 2004;556:249–252.

8. Shigemura N, Okumura M, Mizuno S, Imanishi Y, Nakamura T, Sawa Y. Autologous transplantation of adipose tissue-derived stromal cells ameliorates pulmonary emphysema. *Am J Transplant* 2006;6:2592–2600.

9. Zuk PA, Zhu M, Mizuno H, Huang J, Futrell JW, Katz AJ, Benhaim P, Lorenz HP, Hedrick MH. Multilineage cells from human adipose tissue: implications for cell-based therapies. *Tissue Eng* 2001;7:211–228.

10. Rehman J, Li J, Parvathaneni L, Karlsson G, Panchal VR, Temm CJ, Mahenthiran J, March KL. Exercise acutely increases circulating endothelial progenitor cells and monocyte-/macrophage-derived angiogenic cells. *J Am Coll Cardiol* 2004;43:2314–2318.

11. Rajashekhar G, Traktuev DO, Roell WC, Johnstone BH, Merfeld-Clauss S, Van Natta B, Rosen ED, March KL, Clauss M. Ifats collection: adipose stromal cell differentiation is reduced by endothelial cell contact and paracrine communication. Role of canonical WNT signaling. *Stem Cells* 2008;26:2674–2681.

12. Cai L, Johnstone BH, Cook TG, Tan J, Fishbein MC, Chen PS, March KL. Ifats collection: human adipose tissue-derived stem cells induce angiogenesis and nerve sprouting following myocardial infarction, in conjunction with potent preservation of cardiac function. *Stem Cells* 2009;27:230–237.

13. Rodriguez AM, Pisani D, Dechesne CA, Turc-Carel C, Kurzenne JY, Wdziekonski B, Villageois A, Bagnis C, Breittmayer JP, Groux H, *et al.* Transplantation of a multipotent cell population from human adipose tissue induces dystrophin expression in the immunocompetent MDX mouse. *J Exp Med* 2005;201:1397–1405.

14. Wei X, Zhao L, Zhong J, Gu H, Feng D, Johnstone BH, March KL, Farlow MR, Du Y. Adipose stromal cells-secreted neuroprotective media against neuronal apoptosis. *Neurosci Lett* 2009;462:76–79.

15. Traktuev DO, Prater DN, Merfeld-Clauss S, Sanjeevaiah AR, Saadatzadeh MR, Murphy M, Johnstone BH, Ingram DA, March KL. Robust functional vascular network formation in vivo by cooperation of adipose progenitor and endothelial cells. *Circ Res* 2009;104:1410–1420.

16. Guerassimov A, Hoshino Y, Takubo Y, Turcotte A, Yamamoto M, Ghezzo H, Triantafillopoulos A, Whittaker K, Hoidal JR, Cosio MG. The development of emphysema in cigarette smoke-exposed mice is strain dependent. *Am J Respir Crit Care Med* 2004;170:974–980.

17. Bartalesi B, Cavarra E, Fineschi S, Lucattelli M, Lunghi B, Martorana PA, Lungarella G. Different lung responses to cigarette smoke in two strains of mice sensitive to oxidants. *Eur Respir J* 2005;25:15–22.

18. Agusti AG, Noguera A, Sauleda J, Sala E, Pons J, Busquets X. Systemic effects of chronic obstructive pulmonary disease. *Eur Respir J* 2003;21:347–360.

19. Oudijk EJ, Lammers JW, Koenderman L. Systemic inflammation in chronic obstructive pulmonary disease. *Eur Respir J Suppl* 2003;46:5s–13s.

20. Gosker HR, Langen RC, Bracke KR, Joos GF, Brusselle GG, Steele C, Ward KA, Wouters EF, Schols AM. Extrapulmonary manifestations of chronic obstructive pulmonary disease in a mouse model of chronic cigarette smoke exposure. *Am J Respir Cell Mol Biol* 2009;40:710–716.

21. Rabkin S, Boyko E, Streja D. Relationship of weight loss and cigarette smoking to changes in high-density lipoprotein cholesterol. *Am J Clin Nutr* 1981;34:1764–1768.

22. Serobyan N, Orlovskaya I, Kozlov V, Khaldoyanidi SK. Exposure to nicotine during gestation interferes with the colonization of fetal bone marrow by hematopoietic stem/progenitor cells. *Stem Cells Dev* 2005;14:81–91.

23. Serobyan N, Schraufstatter IU, Strongin A, Khaldoyanidi SK. Nicotinic acetylcholine receptor-mediated stimulation of endothelial cells results in the arrest of haematopoietic progenitor cells on endothelium. *Br J Haematol* 2005;129:257–265.

24. Traktuev DO, Merfeld-Clauss S, Li J, Kolonin M, Arap W, Pasqualini R, Johnstone BH, March KL. A population of multipotent CD34-positive adipose stromal cells share pericyte and mesenchymal surface markers, reside in a periendothelial location, and stabilize endothelial networks. *Circ Res* 2008;102:77–85.

25. Soriano P. Generalized lacz expression with the ROSA26 CRE reporter strain. *Nat Genet* 1999;21:70–71.

26. Tuder RM, Zhen L, Cho CY, Taraseviciene-Stewart L, Kasahara Y, Salvemini D, Voelkel NF, Flores SC. Oxidative stress and apoptosis

interact and cause emphysema due to vascular endothelial growth factor receptor blockade. *Am J Respir Cell Mol Biol* 2003;29:88–97.

27. Aherne WA, Dunnill MS. Morphometry. London: E. Arnold; 1982.

28. Broxmeyer HE, Orschell CM, Clapp DW, Hangoc G, Cooper S, Plett PA, Liles WC, Li X, Graham-Evans B, Campbell TB, *et al.* Rapid mobilization of murine and human hematopoietic stem and progenitor cells with AMD3100, a CXCR4 antagonist. *J Exp Med* 2005;201:1307–1318.

29. Cooper S, Broxmeyer HE. Current protocols in immunology. New York: John Wiley & Sons; 1996.

30. Carp H, Janoff A. Inactivation of bronchial mucous proteinase inhibitor by cigarette smoke and phagocyte-derived oxidants. *Exp Lung Res* 1980;1:225–237.

31. Liu X, Kohyama T, Kobayashi T, Abe S, Kim H, Reed EC, Rennard SI. Cigarette smoke extract inhibits chemotaxis and collagen gel contraction mediated by human bone marrow osteoprogenitor cells and osteoblast-like cells. *Osteoporos Int* 2003;14:235–242.

32. Pandit TS, Sikora L, Muralidhar G, Rao SP, Sriramarao P. Sustained exposure to nicotine leads to extramedullary hematopoiesis in the spleen. *Stem Cells* 2006;24:2373–2381.

33. Lee EY, Xia Y, Kim W, Kim M, Kim T, Kim K, Park B, Sung J. Hypoxia-enhanced wound-healing function of adipose-derived stem cells: increase in stem cell proliferation and up-regulation of VEGF and BFGF. *Wound Repair Regen* 2009;17:540–547.

34. Wang JH, Liu N, Du HW, Weng JS, Chen RH, Xiao YC, Zhang YX. Effects of adipose-derived stem cell transplantation on the angiogenesis and the expression of BFGF and VEGF in the brain post focal cerebral ischemia in rats [in Chinese]. *Xi Bao Yu Fen Zi Mian Yi Xue Za Zhi* 2008;24:958–961.

35. Moy AB, Van Engelenhoven J, Bodmer J, Kamath J, Keese C, Giaever I, Shasby S, Shasby DM. Histamine and thrombin modulate endothelial focal adhesion through centripetal and centrifugal forces. *J Clin Invest* 1996;97:1020–1027.

36. Rangasamy T, Cho CY, Thimmulappa RK, Zhen L, Srisuma SS, Kensler TW, Yamamoto M, Petrache I, Tuder RM, Biswal S. Genetic ablation of NRF2 enhances susceptibility to cigarette smoke-induced emphysema in mice. *J Clin Invest* 2004;114:1248–1259.

37. Kang MJ, Lee CG, Cho SJ, Homer RJ, Elias JA. IFN-gamma-dependent DNA injury and/or apoptosis are critical in cigarette smoke-induced murine emphysema. *Proc Am Thorac Soc* 2006;3:517–518.

38. Hoffman AM, Shifren A, Mazan MR, Gruntman AM, Lascola KM, Nolen-Walston R, Kim CF, Tsai L, Pierce RA, Mecham RP, *et al.* Matrix modulation of compensatory lung regrowth and progenitor cell proliferation in mice. *Am J Physiol Lung Cell Mol Physiol* 2010;298:L158–L168.

39. Hegab AE, Kubo H, Yamaya M, Asada M, He M, Fujino N, Mizuno S, Nakamura T. Intranasal HGF administration ameliorates the physiologic and morphologic changes in lung emphysema. *Mol Ther* 2008;16:1417–1426.

40. Shigemura N, Okumura M, Mizuno S, Imanishi Y, Matsuyama A, Shiono H, Nakamura T, Sawa Y. Lung tissue engineering technique with adipose stromal cells improves surgical outcome for pulmonary emphysema. *Am J Respir Crit Care Med* 2006;174:1199–1205.

41. Zhao Y, Ohkawara H, Rehman J, Wary K, Vogel S, Minshall R, Zhao Y, Malik A. Bone marrow progenitor cells induce endothelial adherens junction integrity by sphingosine-1-phosphate–mediated RAC1 and CDC42 signaling. *Circ Res* 2009;105:696–704.

42. Di Francia M, Barbier D, Mege JL, Orehek J. Tumor necrosis factor-alpha levels and weight loss in chronic obstructive pulmonary disease. *Am J Respir Crit Care Med* 1994;150:1453–1455.

43. Gimble J, Guilak F. Adipose-derived adult stem cells: isolation, characterization, and differentiation potential. *Cytotherapy* 2003;5:362–369.

44. Aust L, Devlin B, Foster SJ, Halvorsen YD, Hicok K, du Laney T, Sen A, Willingmyre GD, Gimble JM. Yield of human adipose-derived adult stem cells from liposuction aspirates. *Cytotherapy* 2004;6:7–14.

45. Lee RH, Pulin AA, Seo MJ, Kota DJ, Ylostalo J, Larson BL, Semprun-Prieto L, Delafontaine P, Prockop DJ. Intravenous HMSCS improve myocardial infarction in mice because cells embolized in lung are activated to secrete the anti-inflammatory protein TSG-6. *Cell Stem Cell* 2009;5:54–63.

46. Van Eeden S, Yeung A, Quinlam K, Hogg JC. Systemic response to ambient particulate matter relevance to chronic obstructive pulmonary disease. *Proc Am Thorac Soc* 2005;2:61–67.